Open Access Journal

Journal of Power Technologies 99 (4) (2019) 264–271

journal homepage:papers.itc.pw.edu.pl

A Novel Dual Input High-Step up DC-DC Converter with One Bi-directional Port for Renewables

Mohammad Amin Bagherpour[a], Payam Farhadi[b,*], Nazanin Bagherpour Hassanlouei[c]

[a] *Department of Electrical Engineering, Tabriz Branch, Islamic Azad University, Tabriz, Iran;*
[b] *Young Researchers and Elite Club, Parsabad Moghan Branch, Islamic Azad University, Parsabad Moghan, Iran;*
[c] *Universita Degli Studi Milano, Milan, Italy;*

Abstract

In this paper, a novel dual-input high step DC-DC converter is developed. The structure of proposed converter consists of one unidirectional and one bidirectional port. The bidirectional port is connected to a battery for energy balancing purpose. That is, the battery stores extra produced energy and/or releases stored energy in situations where there is a lack of energy. On the other hand, the bidirectional port is employed as the main power source. The high step-up output voltage gain of the proposed converter makes it suitable for renewable energy applications where the output voltage is low. The proposed structure is superior over the previously proposed ones in terms of the number of components, energy interaction, simple configuration, and flexibility. The experimental results obtained in three different modes (i.e., without battery, with battery charging, and with battery discharging) are presented to verify the theoretical analysis and the performance of the proposed converter.

Keywords: Bidirectional port, DC-DC Converter, High Step-up, Renewables

1. Introduction

In recent years, due to the expanding use of renewable energy sources like PV, FC, wind, etc., designing new converters with appropriate control methods to reflect the variability of the resources is critical [4, 9]. Due to the characteristics of renewable energy sources, they need to be used in parallel with other resources. For example, photovoltaic (PV) panels are unable to supply load at night. Moreover, the rate of energy produced varies according to insolation and temperature. Most renewable energy output voltage is very low and variable. To deal with the aforementioned problems, most renewable energy resources need high step-up converters to run alongside them [11].

In order to increase the efficiency of renewable energy sources, multi-input converters are introduced [2, 3, 6, 7, 12]. In [12] a dual input DC-DC converter is presented. One key benefit of this converter is individual control of the source to provide the desired voltage at the output and MPP (Maximum Power Point) for inputs. An improved structure of dual input DC-DC converter is introduced in [2]. Compared to [12] the proposed converter in [2] has better output voltage gain and resolves some of the drawbacks of the converters in [12]. The converters proposed in [3, 6, 7] are mostly modular with a high number of power sources and switches. In these circuit structures, each module uses an individual power switch for control. The power source's energy is transferred to load by an individual inductor of the energy source.

As mentioned earlier, most renewable energy sources generate low value voltage. High gain DC-DC converters are offered in two basic groups, converters with coupled inductors and low numbers of circuit elements and circuits without coupled inductors with a high number of circuit elements. [8, 10] offer two high

*Corresponding author
Email addresses: ma.baqerpour@gmail.com (Mohammad Amin Bagherpour), pa.farhadi@gmail.com (Payam Farhadi)

gain DC-DC converters, with and without using coupled inductor. [8] presents a coupled inductor based high gain DC-DC converter. In this structure output, voltage gain can be changed by varying the transformer ratio. The proposed converter in [10] is a high gain DC-DC converter. In this circuit voltage gain is increased without using coupled inductor, but the high number of power switches and circuit components can be viewed as drawbacks.

The recently proposed high gain multi input DC-DC converter and PDFCM [1, 5] are good for use in renewable energy sources. The high step-up capability makes this structure flexible for use across wide voltage ranges. Also by having a multi input circuit, the efficiency of the converter is increased by making it reliable for use off grid. In this paper, a high step up multi input DC-DC converter is proposed. In addition to the benefits that were mentioned for high gain and multi input converters, the proposed converter consists of two ports, a unidirectional and a bidirectional. Having a bidirectional port provides an opportunity to use a battery in the converter structure to save extra produced power and to supply load when the generated energy is too low to be individually supplied by the main energy source.

2. Operational Principles

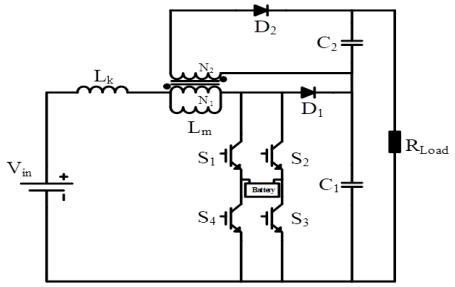

Figure 1: Circuit structure of the proposed converter

Fig. 1 shows the circuit structure of the proposed converter. It consists of four power switches (S_1, S_2, S_3, and S_4), two diodes (D_1 and D_2), two capacitors (C_1 and C_2), magnetizing and leakage inductors (L_m and L_k), and load (R_{Load}). The converter is operated in three operation modes:

1. Without Battery,
2. Battery Charging,
3. Battery Discharging.

Each mode operation is divided into sub-modes as described below.

2.1. Without battery (Mode-I)

Operation sub-modes of the converter in mode one are depicted in Fig. 2. The equivalent waveform of the proposed converter in this mode is also shown in Fig. 3.

***First Sub-Mode [$t_0 - t_1$]*:** This mode starts by turning on switches S_1, S_4 or S_2, S_3. Due to the difference in leakage and magnetizing inductors' current value, diode D_2 conducts. Leakage and magnetizing inductors' current difference charge capacitor C_2 on the secondary side of the coupled inductor. Magnetizing inductor's current decreases due to the negative voltage on it, but the leakage inductor's stored energy increases.

***Second Sub-Mode [$t_1 - t_2$]*:** This sub-mode starts when leakage and magnetizing inductors' stored energy become equal with each other and diode D_2 is turned off. This sub-mode lasts until the power switches turn off.

***Third Sub-Mode [$t_2 - t_3$]*:** This sub-mode starts when the power switches turn off. In this sub-mode, the switches' parallel capacitors start to be charged by turning the power switches off. The capacitors continue charging until the switches' parallel capacitors voltage reaches capacitor C_1's. In this mode the inductors' stored energy decreases and this mode finishes when diode D_1 and D_2 conduct.

***Fourth Sub-Mode [$t_3 - t_4$]*:** In this sub-mode, each of the leakage and magnetizing inductors face different parallel voltages. The difference between the inductors' current is transferred to the secondary side of the coupled inductor to charge capacitor C_2. Capacitor C_1 charges with leakage inductors' current and this sub-mode lasts until the power switches turn on.

Fig. 3 shows some of the waveforms of the proposed converter in mode one. The wave forms include power switches turning on and off times, input current, magnetizing inductor current and diodes current. In order to calculate the output voltage's gain of the proposed converter the following condition is assumed:

1. Proposed converter operates in continuous conduction mode (CCM);
2. Due to the small size of the leakage inductor, it is not considered in calculations.

Eq. (1) is a general assumption in proposed converter calculations.

$$V_O = V_{C1} + V_{C2} \tag{1}$$

where V_O, V_{C1} , and V_{C2} are output voltage, first capacitor's voltage and second capacitor's voltage, respectively.

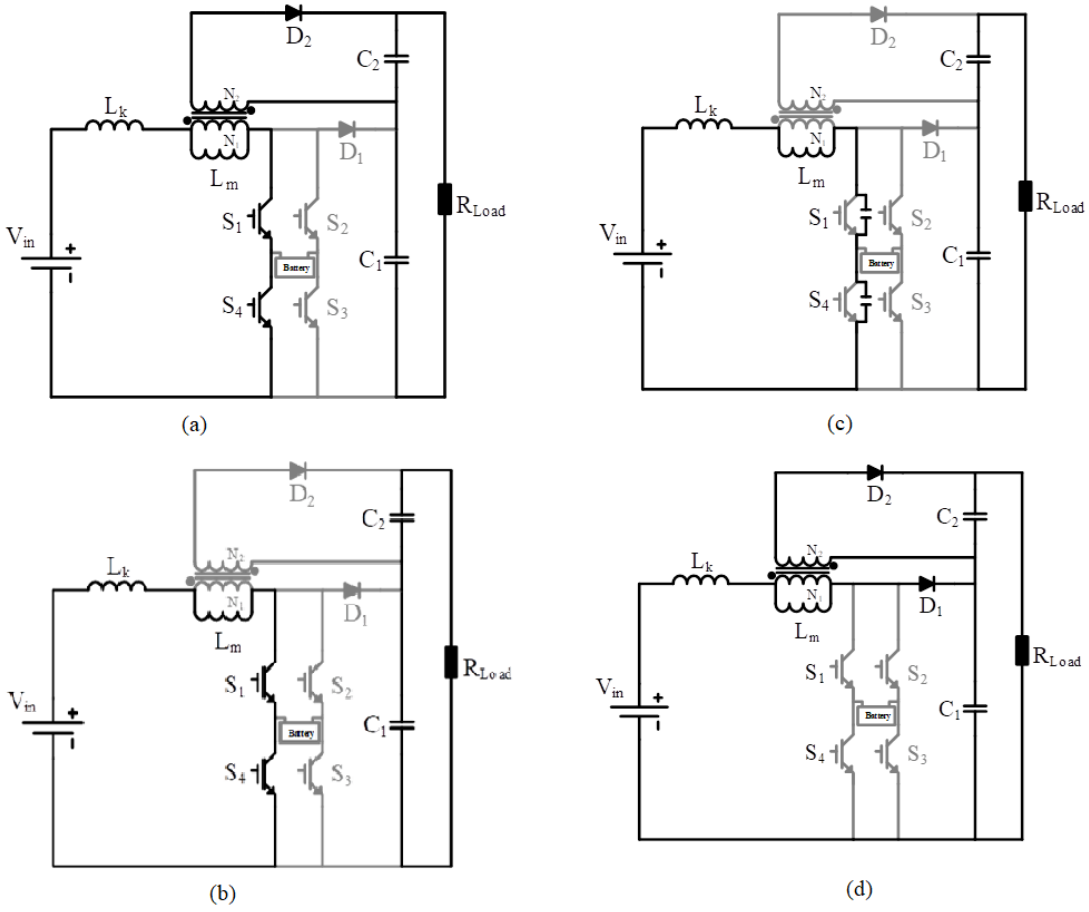

Figure 2: Sub-modes of the proposed converter in mode-I: (a) [t_0-t_1], (b) [t_1-t_2], (c) [t_2-t_3], (d) [t_3-t_4]

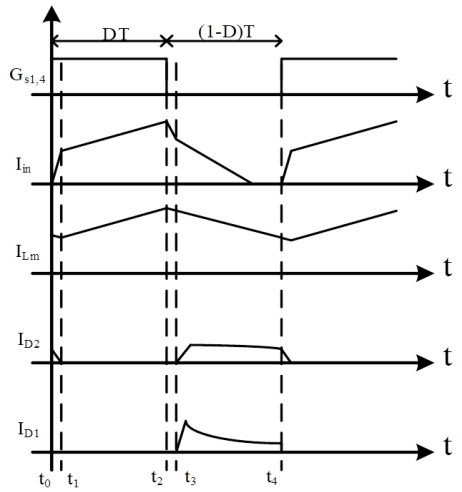

Figure 3: The proposed converter's equivalent waveforms in mode-I

In mode one, consideration is not given to sub-mode one and sub-mode three in calculations due to their small and unimportant size. In DT interval, D is equal to duty cycle and T stands for the period of the switching, giving:

$$V_{Lm} = V_{in} \tag{2}$$

where V_{Lm} and V_{in} are magnetizing inductor's voltage and input voltage, respectively.

And, in (1-D)T interval:

$$V_{Lm} = V_{in} - V_{C1} \tag{3}$$

$$V_{Lm} = -\frac{N_1}{N_2} V_{C2} \tag{4}$$

Using (2), (3) and (4), the following relationship can be obtained:

$$V_{C1} = \frac{V_{in}}{1-D} \tag{5}$$

$$V_{C2} = \frac{\frac{N_2}{N1} D V_{in}}{1-D} \tag{6}$$

At the end, by using (1), (5) and (6) output voltage gain is:

$$V_O / V_{in} = (1 + (N_2/N_1)D)/(1-D) \tag{7}$$

2.2. Battery charging (Mode II)

In this mode extra produced energy is stored in the battery. Sub-modes of the converter in this mode are illustrated in Fig. 4. Wave forms of the converter in this mode is depicted in Fig. 5.

***First Sub-Mode [$t_0 - t_1$]*:** This mode starts by turning on switches S_1, S_4 or S_2, S3. Just same as first sub-mode of mode one, due to difference in leakage and magnetizing inductors current value, diode D_2 conducts. Leakage and magnetizing inductors current difference charges capacitor C_2 on the secondary side of the coupled inductor. Magnetizing inductors' current decreases due to the negative voltage on it; but the, leakage inductors' stored energy increases.

***Second Sub-Mode [$t_1 - t_2$]*:** This sub-mode is the same as the respective sub-mode of mode one and it starts when leakage and magnetizing inductors' stored energy become equal with each other and diode D2 turns off. This sub-mode lasts until the power switches turn off.

***Third Sub-Mode [$t_2 - t_3$]*:** By turning switch S_4 off and turning switch S_3 on, this sub-mode starts. In this sub-mode the power source energy transfers to the battery and leakage and magnetizing inductors charge with lower slope (assuming the power source voltage is higher than the battery voltage).

***Fourth Sub-Mode [$t_3 - t_4$]*:** To start this sub-mode, the power switches turns off. In this sub-mode, the switches' parallel capacitors start to charge by turning the power switches off. The capacitors continue charging until the switches' parallel capacitors' voltage reach that of capacitor C_1's. In this mode inductors' stored energy decreases and this mode finishes when diode D_1 and D_2 conduct.

***Fifth Sub-Mode [$t_4 - t_5$]*:** As in the previous mode, in this sub-mode, each of the leakage and magnetizing inductors face different parallel voltages. The difference of the inductors' current transfers to the secondary side of the coupled inductor to charge capacitor C_2. Capacitor C_1 charges with leakage inductors' current and this sub-mode lasts until the power switches turn on.

The waveforms of the proposed converter in mode two are depicted in Fig. 5. D_1 and D_2 are the equivalent duty cycle of the proposed converter for charging the inductors without battery and with battery, respectively. In Fig. 5, Iin stands for input current, I_{Lm} stands for current flowing through the magnetizing inductor, and ID_1 and ID_2 stand for current flowing through diodes.

In order to calculate the output voltage's gain in this mode, assumptions of Mode-I are valid.

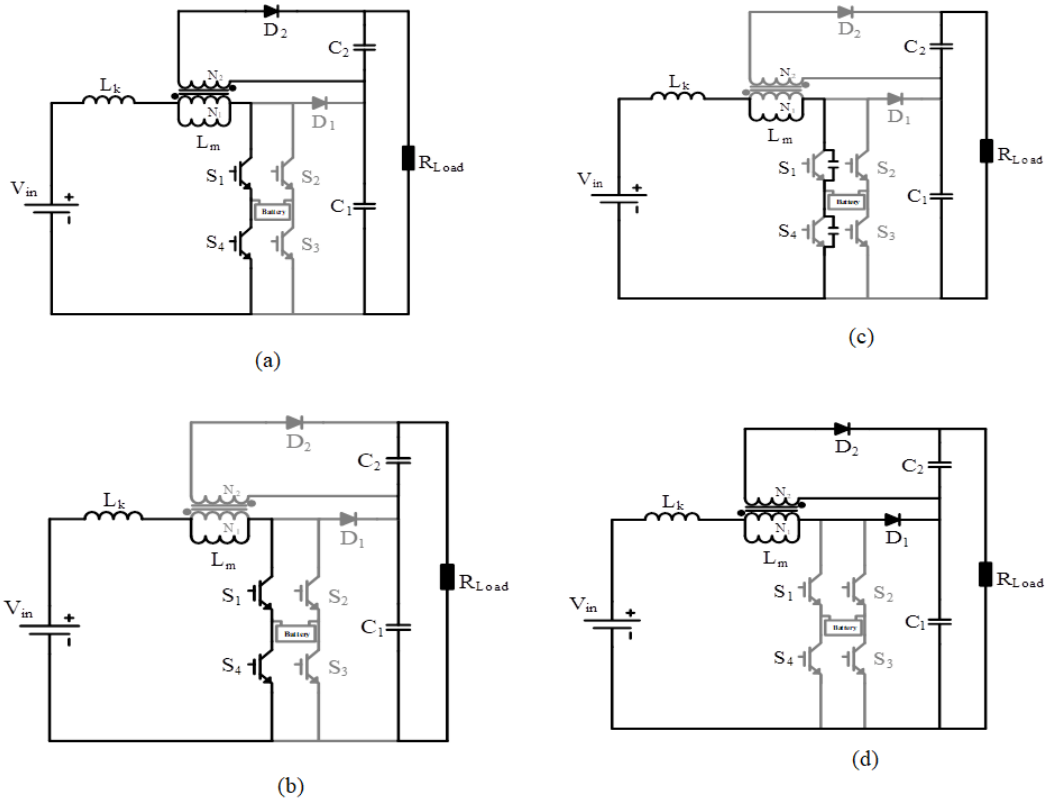

Figure 4: Sub-modes of the proposed converter in mode-II: (a) [t_0-t_1], (b) [t_1-t_2], (c) [t_2-t_3], (d) [t_3-t_4] , (e) [t_4-t_5]

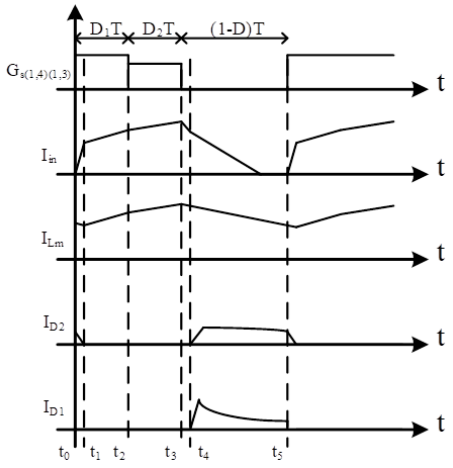

Figure 5: The proposed converter's equivalent waveforms in mode-II

For interval D_1+D_2, we have:

$$V_{Lm} = (D_1 + D_2)V_{in} - D_2 V_{Battery} \tag{8}$$

And for interval 1-(D1+D2), we have:

$$V_{Lm} = V_{in} - V_{C1} \tag{9}$$

$$V_{Lm} = -\frac{N_1}{N2} V_{C2} \tag{10}$$

Using (8), (9) and (10) results in:

$$V_{C1} = \frac{V_{in} - D_2 V_{Battery}}{1 - D_1 - D_2} \tag{11}$$

$$V_{C2} = \frac{\frac{N_2}{N1}}{1 - D_1 - D_2} \left[V_{in}(D_1 + D_2) - D_2 V_{Battery} \right] \tag{12}$$

Finally, by using (1), (11) and (12) output voltages gain in mode two is calculated as:

$$V_O = \frac{V_{in}\left[1 + \frac{N_2}{N1}(D_1 + D_2)\right] - V_{Battery} D_2 \left[\frac{N_2}{N1} + 1\right]}{1 - D_1 - D_2} \tag{13}$$

2.3. Battery discharging (Mode-III)

In this mode, the power source is assumed to be unable to provide the load's required energy and the battery is responsible for supplying the rest of the required energy. For instance, the supply shortage may include PV during night time or very high and/or very low wind

velocities for wind turbines, etc. Waveforms of the proposed converter are depicted in Fig. 6.

***First Sub-Mode [$t_0 - t_1$]*:** This mode starts by turning on switches S_1, S_4 or S_2, S_3. Just same as first sub-mode of mode one and mode two, due to difference in leakage and magnetizing inductors current value, diode D_2 conducts. Leakage and magnetizing inductors' current difference charges capacitor C_2 at the secondary side of the coupled inductor. Magnetizing inductors current decrease due to negative voltage on it; however, leakage inductors stored energy increase.

***Second Sub-Mode [$t_1 - t_2$]*:** This sub-mode starts when leakage and magnetizing inductors' stored energy become equal with each other and diode D_2 is turned off as in mode one and mode two. This sub-mode lasts until the power switches turn off.

***Third Sub-Mode [$t_2 - t_3$]*:** By turning off switch S_1 and turning on switch S_2 this sub-mode starts. In this sub-mode, the power source and battery charge and leakage and magnetizing inductors with higher slope.

***Fourth Sub-Mode [$t_3 - t_4$]*:** This sub-mode starts when the power switches turn off. Switches' parallel capacitors start to charge by turning the power switches off. The capacitors continue charging until the switches' parallel capacitors' voltage reach that of capacitor C_1's. In this mode the inductors' stored energy decreases and this mode finishes when diode D_1 and D_2 conduct.

***Fifth Sub-Mode [$t_4 - t_5$]*:** As in previous modes, in this sub-mode, each of the leakage and magnetizing inductors face different parallel voltages. The difference of the inductors' current transfers to the secondary side of the coupled inductor to charge capacitor C_2. Capacitor C_1 charges with leakage inductors' current and this sub-mode lasts until the power switches turn on.

Fig. 7 shows waveforms of the converter in mode three. D_1 and D_2 are inductors' charging duty cycle without battery and with battery discharging respectively.

For D_1+D_2 interval, we have:

$$V_{Lm} = (D_1 + D_2)\, V_{in} + D_2 V_{Battery} \tag{14}$$

In addition, for 1- D_1-D_2 interval we have:

$$V_{Lm} = V_{in} - V_{C1} \tag{15}$$

$$V_{Lm} = -\frac{N_1}{N2} V_{C2} \tag{16}$$

The following relationship can be gained by using (14), (15) and (16):

$$V_{C1} = \frac{V_{in} + D_2 V_{Battery}}{1 - D_1 - D_2} \tag{17}$$

$$V_{C2} = \frac{\frac{N_2}{N1}}{1 - D_1 - D_2} \left[V_{in}\,(D_1 + D_2) + D_2 V_{Battery} \right] \tag{18}$$

Output voltage gain of the proposed converter in Mode-III can be calculated using (1), (17) and (18) as follows:

$$V_O = \frac{V_{in} \left[1 + \frac{N_2}{N1}\,(D_1 + D_2) \right] + V_{Battery} D_2 \left[\frac{N_2}{N1} + 1 \right]}{1 - D_1 - D_2} \tag{19}$$

3. Experimental Results

In order to verify performance of the proposed converter, an experimental circuit is investigated. The performance of the converter in experimental research is divided into three modes, reflecting the performance principles. The switching frequency of the proposed converter in this research is about 30 kHz and the voltages of the input and battery are 20 V and 15 V respectively. Load is about 100 V for all of the experimental tests and we tested the proposed converter on its capability to provide all three modes. Fig 8 shows the performance of the converter in the first mode (Without Battery). From up to down wave forms are output voltage, input current, diode D_2's current and diode D_1's current. According to equation (7), out voltage of the proposed converter in this mode considering $D = 1/3$ should be 140 V which the experimental results verify. Input current is about 12 A in its peak and waveform is similar to expected results in Fig. 3. Diode D_1, 2s' currents are similar to presumed waveforms in Fig. 3 and are about 5 A and 10 A at their peak respectively.

Experimental results for the second mode (Battery Charging) is depicted in Fig. 9. In this mode D_1 = 1/3 and D_2 = 1/3, which results in 95 V according to (13). Experimental results in Fig. 9 verify performance of the converter in this mode. In Fig. 9 wave forms are ordered similar to the first mode (Fig. 8). As was expected, input current, diode D_2 current and diode D_1 current are similar to waveforms in Fig. 5. Input's, diode D_2's and diode D_1's currents at their peaks are 8 A, 4 A and 6 A, respectively.

Fig. 10 shows experimental results for the third mode (Battery Discharging). In this mode wave forms are ordered similarly to the previous results. The proposed converter operates with D_1 = 1/3 and D_2 = 1/3 in this

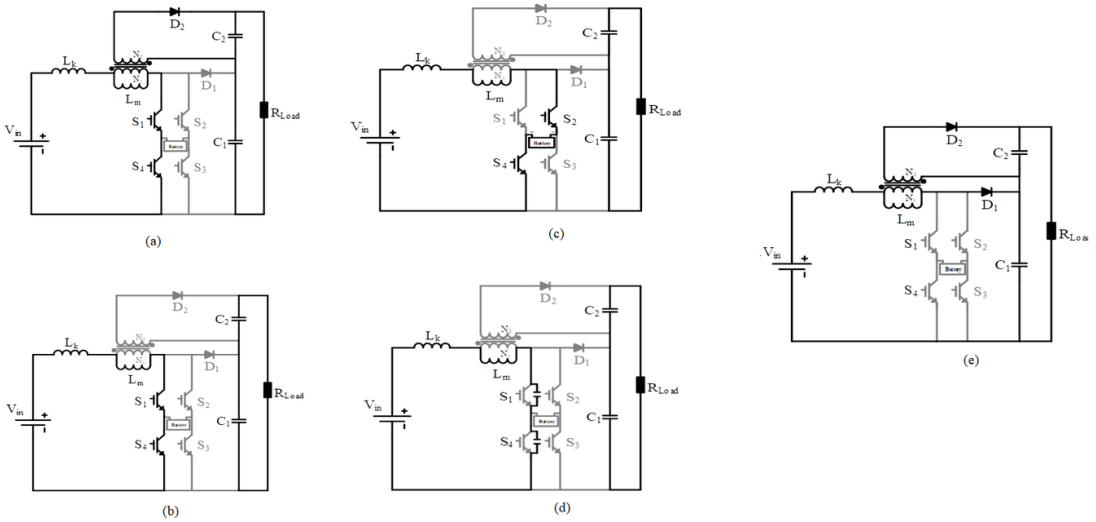

Figure 6: Sub-modes of the proposed converter in mode-III: (a) [t_0-t_1], (b) [t_1-t_2], (c) [t_2-t_3], (d) [t_3-t_4] , (e) [t_4-t_5]

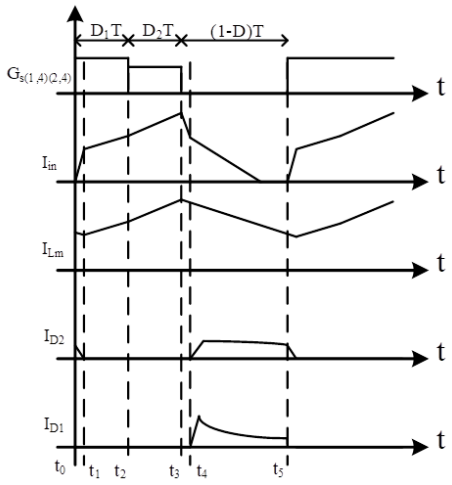

Figure 7: The proposed converter's equivalent waveforms in mode-III

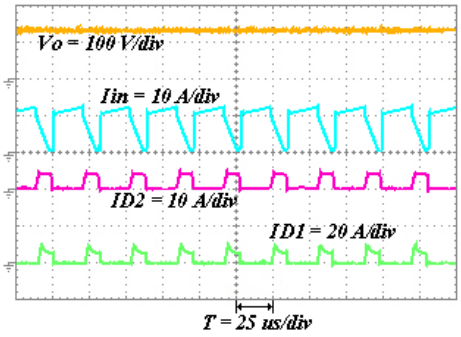

Figure 8: Experimental results for proposed converter in mode-I

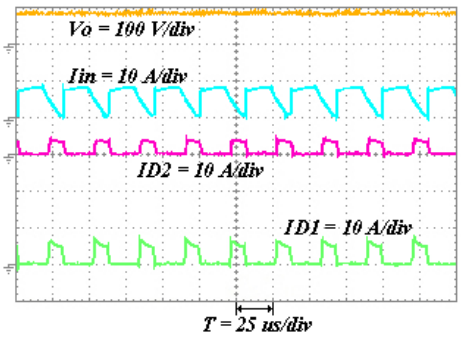

Figure 9: Experimental results for proposed converter in mode-II

mode. Equation (19) shows that the output voltage in this mode is 185 V, which experimental results verify. In this mode input's, diode D_2's and diode D_1's currents are 18 A, 8 A and 12 A at their peaks respectively. Waveforms are similar to Fig. 7 as was expected.

4. Conclusion

In this paper, a newly developed high step-up double input DC-DC converter was presented. The performance of the proposed converter was evaluated in three different modes (namely, without battery, with battery charging, and with battery discharging). In addition, operation of the presented structure in each of the modes was described and equivalent equations were calculated. In order to verify the theoretical performance of the converter, the experimental results were also provided. The results are very consistent both in theory and experiment.

[1] Masoud Afsharikhamaneh, Payam Farhadi, Mostafa Abarzadeh, Jaber Ebrahimi, and Tina Sojoudi. Structure for double flying capacitor multicell converter progressive double flying capacitor multicell converter. *IET Power Electronics*,

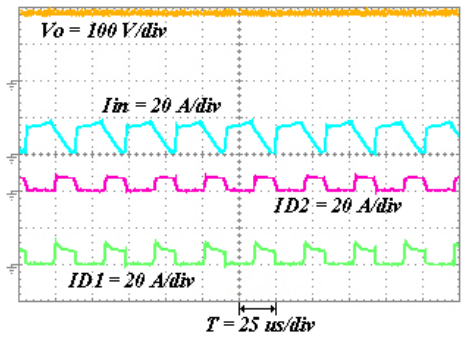

Figure 10: Experimental results for proposed converter in mode-III

8(2):297–308, feb 2015.

[2] Mohammad Reza Banaei, Hossein Ardi, Rana Alizadeh, and Amir Farakhor. Non-isolated multi-input–single-output DC/DC converter for photovoltaic power generation systems. *IET Power Electronics*, 7(11):2806–2816, nov 2014.

[3] Hamid Behjati and Ali Davoudi. Single-stage multi-port DC–DC converter topology. *IET Power Electronics*, 6(2):392–403, feb 2013.

[4] Chien-Liang Chen, Yubin Wang, Jih-Sheng Lai, Yuang-Shung Lee, and D. Martin. Design of Parallel Inverters for Smooth Mode Transfer Microgrid Applications. *IEEE Transactions on Power Electronics*, 25(1):6–15, jan 2010.

[5] Yen-Mo Chen, Alex Q. Huang, and Xunwei Yu. A High Step-Up Three-Port DC–DC Converter for Stand-Alone PV/Battery Power Systems. *IEEE Transactions on Power Electronics*, 28(11):5049–5062, nov 2013.

[6] Saeed Danyali, Seyed Hossein Hosseini, and Gevorg B. Gharehpetian. New Extendable Single-Stage Multi-input DC–DC/AC Boost Converter. *IEEE Transactions on Power Electronics*, 29(2):775–788, feb 2014.

[7] Serkan Dusmez, Xiong Li, and Bilal Akin. A new multi-input three-level integrated DC/DC converter for renewable energy systems. In *2015 IEEE Applied Power Electronics Conference and Exposition (APEC)*. IEEE, mar 2015.

[8] Yanying Gao, Hongchen Liu, and Jian Ai. Novel High Step-Up DC–DC Converter with Three-Winding-Coupled-Inductors and Its Derivatives for a Distributed Generation System. *Energies*, 11(12):3428, dec 2018.

[9] Y.A.-R.I. Mohamed and E.F. El Saadany. Hybrid Variable-Structure Control With Evolutionary Optimum-Tuning Algorithm for Fast Grid-Voltage Regulation Using Inverter-Based Distributed Generation. *IEEE Transactions on Power Electronics*, 23(3):1334–1341, may 2008.

[10] Gang Wu, Xinbo Ruan, and Zhihong Ye. Nonisolated High Step-Up DC–DC Converters Adopting Switched-Capacitor Cell. *IEEE Transactions on Industrial Electronics*, 62(1):383–393, jan 2015.

[11] Qun Zhao and F.C. Lee. High-efficiency high step-up DC-DC converters. *IEEE Transactions on Power Electronics*, 18(1):65–73, jan 2003.

[12] L.-W. Zhou, B.-X. Zhu, and Q.-M. Luo. High step-up converter with capacity of multiple input. *IET Power Electronics*, 5(5):524, 2012.